

CFD Analysis of Multi-jet Air Impingement on Flat Plate

Chougule N.K., Parishwad G.V., Gore P.R., Pagnis S., Sapali S.N.

Abstract—Jet impingement is one of the intensive cooling methods to cool hot objects in various industrial processes. The fluid flow and heat transfer characteristics of multi air jet array impinging on a flat plate are investigated both experimentally and numerically. It is found that Shear-Stress Transport (SST) k- ω turbulence model can give the better predictions of fluid flow and heat transfer properties for solving such types of problems. Using SST k- ω model, the effects of jet Reynolds number (Re), target spacing-to-jet diameter ratio (Z/d) on average Nusselt number (Nu_a) of the target plate are examined. These numerical results are compared with the available benchmark experimental data. It is found that Nu_a increases from 40 to 50.1 by increasing Reynolds number from 7000 to 11000 at Z/d =6. By increasing Z/d ratio from 6 to 10, Nu_a decreases from 50.1 to 36.41 at Re11000. It is also observed that in multi-jet impingement, spacing between the air jets play important role. A value of nozzle pith of 3 to 5 was recommended to reduce adjacent jet interference.

Index Terms— CFD, heat transfer enhancement, multi jet impingement, turbulence model

I. INTRODUCTION

JET impingement is one of the very efficient solutions of cooling hot objects in industrial processes as it produces a very high heat transfer rate through forced-convection. There is a large class of industrial processes in which jet impingement cooling is applied such as the cooling of blades/vanes in a gas turbine, the quench of products in the steel and glass industries and the enhancement of cooling efficiency in the electronic industry. Over the past 30 years, experimental and numerical investigations of flow and heat transfer characteristics under single or multiple impinging jets remain a very dynamic research area. The effects of nozzle geometry, jet-to-surface spacing, jet-to-jet spacing, cross flow, operating conditions, etc. on flow and heat transfer have been studied by both experimentally and numerically.

Manuscript received Feb 5, 2011; revised Feb 14, 2011.

Chougule NK is Assistant professor in Mechanical Engineering Department at College of Engineering, Pune India phone:+91-02027241; fax:+91—2027255; e-mail: chougulenk@gmail.com

Parishwad G.V and Sapali S.N are Professors in Mechanical Engineering Department at College of Engineering, Pune India e-mail: gcp.mech@coep.ac.in, sns.mech@coep.ac.in

Pagnis S. is Fuel system Analyst with Tata Technologies , Europe sachin.pagnis@gmail.com

Gore P.G. is with EMERSON Network Power, Thane M.S., India goreprashant7@gmail.com

Most industrial applications of impinging jets are concerned with turbulence flow in the whole domain downstream of a nozzle. Modeling of turbulence flow presents the greatest challenge for rapidly and accurately predicting impingement heat transfer even under a single round jet. Over the past decade, although no single model has been universally accepted to be superior to all classes of problems, various turbulence models have been developed successfully to roughly predict impingement flow and heat transfer. However, there are only a limited number of studies concerned with comparisons of the reliability, availability and capability of different turbulence models for impingement flows.

Thakare and Joshi [1] evaluated twelve versions of low Reynolds number k- ϵ models and two low Reynolds number Reynolds stress models (RSM) for heat transfer in turbulence pipe flows. Their comparative analysis between the k- ϵ models and RSM models for the Nusselt number prediction is in favor of the applicability of the k- ϵ models even though the RSM model overcomes the assumption of isotropy and the consistency of turbulence Prandtl number.

Shi et al.[2] presented simulation results for a single semi-confined turbulence slot jet impinging normally on a flat plate. The effects of turbulence models, near wall treatments, turbulence intensity, jet Reynolds number, as well as the type of thermal boundary condition on the heat transfer were studied using the standard k- ϵ and RSM models. Their results indicate that both standard k- ϵ and RSM models predict the heat transfer rates inadequately, especially for low nozzle-to-target spacing. For wall-bounded flows, large gradients of velocities, temperature and turbulence scalar quantities exist in the near wall region and thus to incorporate the viscous effects it is necessary to integrate equations through the viscous sub layer using finer grids with the aid of turbulence models.

Leon F.G.[3] investigated velocity field and turbulence fluctuations in a array of circular jets impinging normally on a plane wall. The measurement indicated that the interaction between the self induced cross flow and the wall jets resulted in the formation of horseshoe type vortices that circumscribe the outer jets of the array. It is also observed that center jet has shortest core and highest turbulence kinetic energy, indicative of the strong interaction with a large number of surrounding jets.

In this paper, a numerical study of multiple (3x3) circular air jet vertically impinging on a flat plate is performed with minimum cross flow arrangement. The paper aims to recommend the most suitable model in

predicting this type of flow through an investigation of the relative performance of different turbulence models and find out the effects of jet Re , Z/d ratio on Nu_a of the target plate. Numerical calculations base on the CFD code ANSYS CFX 11.0 are conducted, the justification of the models are carried out by comparing the numerical results with experimental data.

II. NUMERICAL ANALYSIS

A. Geometry and Boundary Conditions

The solution domain is filled with stagnant air. The three dimensional Navier-Stokes and energy equations with the standard turbulence model are solved using CFD software (ICEM mesher and CFX solver) which are combined with continuity and momentum equations to simulate thermal and turbulence flow fields. The turbulence model used is shear stress transport (SST) k-w model which is found to work the best among the available turbulence models for this flow configuration and is also chosen due to its simplicity, computational economy and wide acceptability. The flow is assumed to be steady, incompressible and three dimensional. The buoyancy and radiation heat transfer effects are neglected and thermo physical properties of the fluid such as density, specific heat and thermal conductivity are assumed to be constant. The schematic diagram of the physical geometry and the computational domain is shown in the following Fig.1.

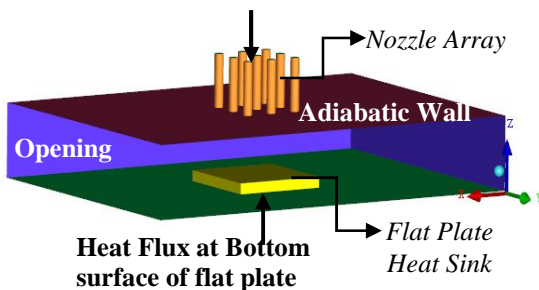


Fig.1 -The computational and Physical domain and Boundary Conditions (BC) of jet impingement

The bottom wall of domain is considered to be bottom surface of heat sink base. It is assumed that heat is generated inside heat sink base at uniform rate and can be represented by a constant heat flux from the bottom surface of the heat sink. If flux coming out of heat sink is not dissipated properly, the temperature of heat sink will go up and it might lead to failure of the component on which heat sink is mounted. Since heat dissipation rates are quite high, natural convection or forced convection by using fans are not enough to cool heat sink. For this we must use finned heat sink with air jet impingement through array of nozzles. Air flow at high velocity passes through a round array jets with length $l=25\text{mm}$ and diameter $d=5\text{mm}$, vertically impinging on the target plate of $60\text{mm} \times 60\text{mm}$ with 6mm thickness. The jet after impingement will exit from opening. The target plate was kept at constant heat input of 30W and except top surface all other walls are adiabatic. The details of nozzle plate geometry are shown in Fig. 2.

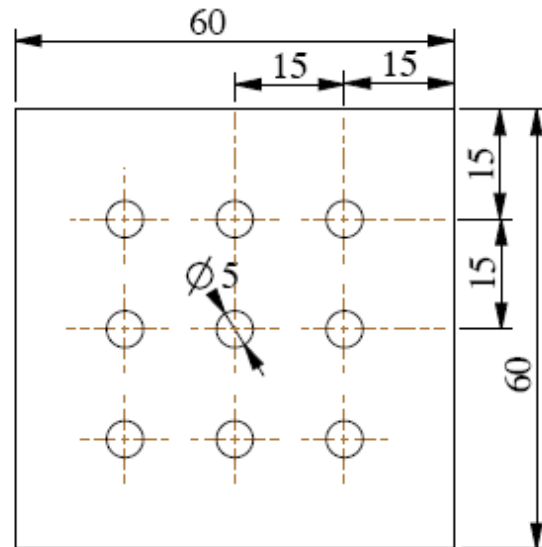


Fig. 2- Geometry of Nozzle Plate

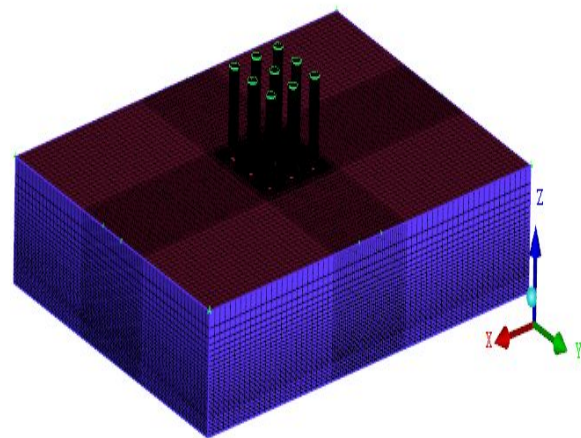


Fig.3- Meshed domain of multi jet impingement

B. Numerical Procedure

As geometry is small enough and we have sufficient computational power so here consider complete geometry for the CFD analyses and created in ANSYS ICEM CFD 11.0. All geometrical dimensions are similar as that of test set up. The opening boundary is sufficiently away from the actual physics so that flow becomes stable and actual flow phenomenon at impinging surface is captured. The structural mesh was created within this domain by using ANSYS ICEM CFD with the option of blocking.

As structured mesh used the orthogonality is maintained, hence accurate prediction of heat transfer characteristics is possible. Hexa mesh is used over the entire computational domain and to predict the near wall flow phenomenon the dense hexa mesh is used as shown in Fig.3. This will not only capture the near wall flow phenomenon but also increase the smoothness of the mesh. Dense mesh also helps to control the y^+ . Grid independency on heat transfer characteristics is checked by changing the element size from 0.15 million to 1.1 million which follows that about 0.72 million was good enough for present analysis from view point of accuracy and computational time.

The numerical simulations are carried out using the

commercial CFD solver ANSYS CFX version 11.0. The flow and turbulence fields have to be accurately solved to obtain reasonable heat transfer predictions. Higher resolution scheme is used for all terms that affect heat transfer. Higher order discretization scheme is used for the pressure; momentum, turbulence kinetic energy, specific dissipation rate, and the energy. Flow, turbulence, and energy equations have been solved. In the fluid domain the inlet boundary condition is specified the measured velocity and static temperature (300K) of the flow were specified at the inlet of the nozzle. No-slip condition was applied to the wall surface. In fluid domain there is also opening boundary condition in which flow regime is subsonic, relative pressure is 0 Pa with the details of operating temperature (300K) and the turbulence intensity of 5%. In solid domain the constant heat flux 8333W/m^2 (30W for 60x60mm plate) was given with the initial temperature condition automatic with 40°C at the base of heat sink and the sides of heat sink base plat are adiabatic. To simplify the solution, the variation of thermal and physical properties of air with temperature is neglected. The flow field was numerically examined by use of CFX (ANSYS), assuming the steady-state flow condition.

C. Solver

A geometry and mesh object is imported into CFX CFD software environment for solving governing equations. The flow and turbulence fields have to be accurately solved to obtain reasonable heat transfer predictions. Second order scheme is used for all terms that affect heat transfer. Second order discretization scheme is used for the pressure; second order upwind discretization scheme is used for momentum, turbulence kinetic energy, specific dissipation rate, and the energy. Flow, turbulence, and energy equations have been solved. To simplify the solution, the variation of thermal and physical properties of air with temperature is neglected. The standard SIMPLE algorithm is adopted for the pressure-velocity coupling. The simulation type is steady state condition, convergence criteria are specified as $10\text{E-}05$ residuals and convergence control is set at maximum 300 iterations which can be changed if convergence is not achieved.

III. EXPERIMENTAL APPARATUS AND PROCEDURES

A schematic of the experimental apparatus is shown in Fig.4. It consists of a 0.5 hp blower, air straightner (air box), contraction section, and structure and DAQ system to measure temperature, pressure. The air is supplied through centrifugal blower, which draws air from the atmosphere and delivers it along a pipe to an air box, which is above the test area. A Honeycomb structure is used inside the air box in order to provide streamlined flow prior to impinging on the heat sink and a butterfly valve used in order to regulate the discharge from the centrifugal blower.

The air flow bench structure is made to incorporate other devices such as DAQ system, Power supply, pressure measurement devices and various controls. Micro-manometer is used to measure the static pressure of air at the outlet of jet at different locations. K-type thermocouples

were used to measure temperature. Average of all the reading will be taken and jet velocity is calculated. After exiting air from air flow bench, it is impinged on target surface. An arrangement has been done to control the distance between the nozzle plate and the heat sink (Z/d ratio), which consists of nozzle plate, heater section, heat sink. The Flat Plate heat sink of aluminum plate with dimension $60\text{mm} \times 60\text{mm} \times 6\text{mm}$ and nozzles of jet diameter 5mm are used for investigation.

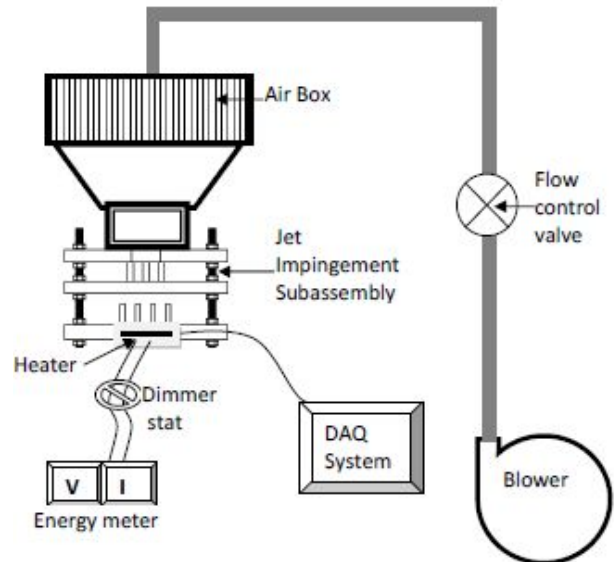


Fig. 4 Experimental setup

Mount the whole jet assembly with air flow bench exit section and connect thermocouple between DAQ system channels and test section. With the help of screw mechanism adjust Z/d ratio. After connecting all circuit and mounting impingement jet assembly to the air flow bench, make heater on to heat the heat sink. Simultaneously start blower to impinge air on the heat sink. Here heat is supplied at the bottom side of the heat sink and except top surface other sides are insulated perfectly. Adjust the dimmer stat in such a way that heat is supplied in the range of 30-50 watts. Measure amount of heat supplied (Q) to heat sink by digital voltmeter (0-230V), ammeter (0-5A). Measure air pressure before and after nozzle plate exit. Based on this pressure drop we can calculate air velocity and Reynolds number. The air velocity is measured using relation $V = C \times \sqrt{2gH}$ where, V is velocity of air jet (m/sec.), g is acceleration due to gravity (m/sec^2), H is manometer level difference (m) and C is coefficient of discharge velocity (0.985). To set at particular Reynolds number butterfly valve is adjusted accordingly. Once flow is adjusted for particular Reynolds number, DAQ system will start on recording temperatures. After getting final steady state condition DAQ system will save the data and exports to the Excel format. Calculate heat sink thermal resistance. Thermal resistance of heat sink is

$$\text{calculated by } R_{th} = \frac{(T_{avg} - T_{\infty})}{Q}$$

IV. RESULT AND DISCUSSION

A. Selection of Turbulence model

Table I shows the comparison of four different turbulence models for jet impingement applications. The results indicate that the SST model provides very good predictions of flow and heat transfer phenomenon at a moderate computational cost.

TABLE I
COMPARISON OF COMMON CFD TURBULENCE MODELS USED FOR IMPINGING JET PROBLEMS

Turbulence Model	Computational Cost (Time in hrs.)	Nu prediction error
k-ε	High (4.52)	Poor: Error 22%
RNG k-ε	Low (3.98)	Poor: Error 18.1%
k-ω	Moderate (4.2)	Good: Error 10%
SST	Moderate (4.3)	Excellent: Error 2.1%

The SST model also predicted mean velocities well, clearly better than the k-ε, RNG k-ε, and k-ω models and within the uncertainty of the experimental measurements. It is also observed that the Nu_a prediction is very good agreement with the experimentation results

B. Validation with Experimental Results

A comparison between experimental and CFD results are shown in Table II. To validate CFD results, the detailed experimentation on same size Aluminum Flat plate is carried out. The average temperature obtained from the experimental data is used to validate the computational work. To simulate the above experimental conditions in context of CFD analysis, the same geometry, boundary conditions are applied and also temperature monitoring points are located at the same position where thermocouples are physically located.

TABLE II
COMPARISON BETWEEN EXPERIMENTAL AND CFD RESULTS

Z/d Ratio	Re number	Experimental Results	CFD results at Experimental points	% error
		h, W/m ²	h, W/m ²	h %
06	7000	221.6	205.3	7.36
06	9000	260.3	239.4	8.06
06	11000	288.6	268.8	6.87
08	7000	179.1	160.6	10.33
08	9000	210.3	192.3	8.53
08	11000	249.8	228.3	8.59
10	7000	155.6	137.9	11.15
10	9000	184.4	165.3	10.37
10	11000	204.6	185.9	9.15

Mostly within all the range of parameters, it is observed that CFD results are in good agreement with experimental results (± 5% error).

C. Effect of Z/d on Heat Transfer

The spread flow is shown by velocity contours in Fig. 5 at Z/d = 6, 8 and 10 for Re 11000. Higher heat transfer is observed for lower Z/d ratio because of reduction in impingement surface area. In case of higher Z/d ratio there is a higher momentum exchange between impinging fluid and quiescent fluid due to this the jet diameter becomes broader and spreads over more surface area. In case of low Z/d ratio the same amount of fluid spreads over lesser surface area causing a higher heat transfer rate.

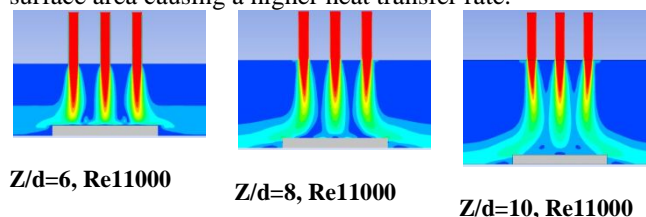


Fig. 5 Velocity contours at Z/d ratio

In case of higher Z/d ratio, there is mixing of jet before impingement which is not desirable and also the outer jets divert outside from the target impingement. At Z/d =6, favorable results are obtained. By increasing Z/d ratio from 6 to 10, Nu_a decreases from 50.1 to 36.41 at Re11000.

D. Effect of Re and Z/d on Temperature Distribution

Fig. 6 shows temperature distribution on the middle cross section of the heat sink with Z/d ratio 6, 8 and 10 and Re 7000, 11000.

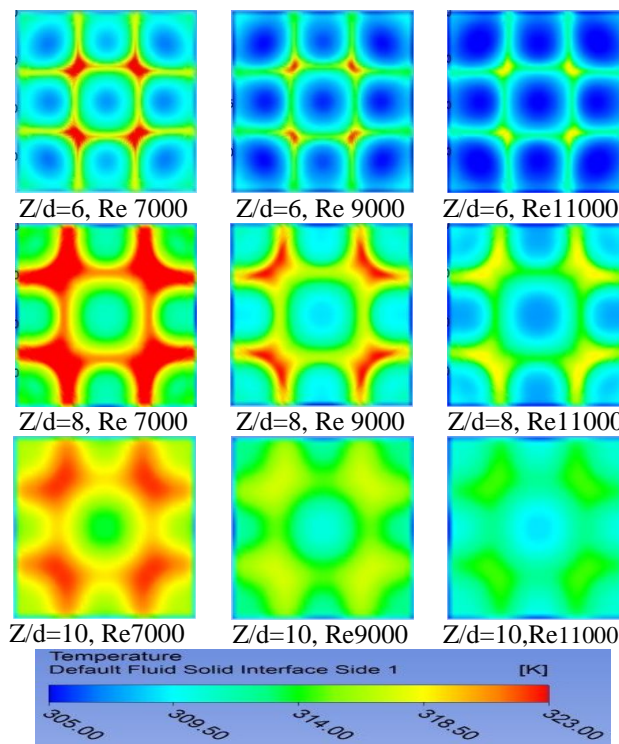


Fig. 6 Temperature distribution on the middle cross section of the heat sink with Z/d ratio 6, 8 and 10 and Re 7000, 11000.

The heat is transferred from the heater to the bottom of the heat sink and is dissipated by convection through fins. The air temperature is higher near the peripheral fins of the heat sink since the air exchanges heat with the heat sink; moreover it is trapped in the recirculation regions. These temperature contour plots shows that for higher Reynolds number, average top surface of flat plate is lower due to localized cooling. It is also observed that the portions of flat plate below nozzle area are cooled intensively than other area. At a particular Re, as Z/d ratio increases the adjacent nozzle flow may mix or become wavier due to which thermal resistance of flat plate increases. Minimum temperature is obtained at stagnation point. Around the central nozzle impingement zone, the higher temperature contours are observed due to cross mixing of flow and intensity of temperature zone at these area increases as we increase Z/d ratio.

Fig.7a shows Position of the line used for the evaluation of local temperature and Fig. 7b illustrates the local temperature distribution along the centerline on the target plate at Z/d=6 and Re=7000, 9000 and 11000. It is observed that as we increase Re, flat plate become cooler. In all cases it is also observed that area below nozzles has lowest temperature compared to other area on the flat plate. Compared to single jet impingement, in multi-jet impingement, more uniform temperature distribution is observed at all the ranges of Re and Z/d ratio.

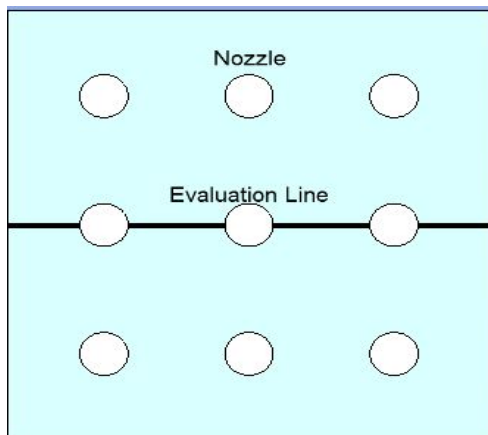


Fig. 7a Position of the line used for the evaluation of local temperature

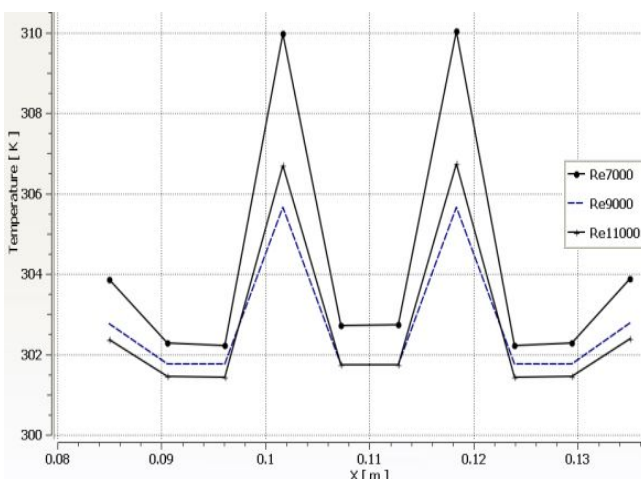


Fig. 7b Local temperature distribution along the centerline

The Nu_a increases from 40 to 50.1 by increasing Reynolds number from 7000 to 11000 at Z/d =6. The average heat transfer coefficient increases with increase in Reynolds number at a given Z/d ratio. At higher Reynolds numbers turbulence level increases and along with this spread of the jet also increases. The net amount of fluid that comes out of the jet is also higher for higher Re which causes better heat transfer performance.

V. CONCLUSIONS

- The SST turbulence model produces better predictions of fluid properties in impinging jet flows and hence recommended.
- There is a very good agreement between experimental results and CFD results ($\pm 5\%$). The present CFD model can be used for wide range of parameter just by changing input parameter without doing exhaustive experimentations.
- Higher heat transfer performance is observed for lower Z/d ratio due to the reduction in the impingement surface area. At Z/d=6, Re =11000, h_{avg} is 268.8 W/m²K.
- Increase in Re increases heat transfer at all given Z/d ratios. By increasing Re from 7000 to 11000 h_{avg} is increased by 24%.
- At a given Re, for higher Z/d ratio outside jets become vibrant and will not impinge at the desired target. Also jets may mix before impingement which is not desirable.
- At Z/d = 6 and Re 9000 comparatively favorable results are observed.

REFERENCES

- [1] Thakare S.S. and Joshi J.B., *CFD modeling of heat transfer in turbulence pipe flows*, Aiche Journal, 2000, Vol.46,pp1798-1812
- [2] Shi Y.L., Ray M.B. and Mujumdar A.S., *Computational study of impingement heat transfer under a turbulence slot jet*, *Industrial & Engineering Chemistry Research*, 2002,Vol.41, pp 4643-4651.
- [3] Leon F.G. et.al, *Experimental investigation of impinging jet arrays*, *Experiments in Fluids*, Springer-Verlag, 2004,36 946-958.
- [4] Bernhard Weigand and Sebastian Spring, 2009, *Multiple Jet Impingement – A Review*, *Int. Symp. on Heat Transfer in Gas Turbine Systems*, Antalya, Turkey
- [5] Martin, H., 1977, *Heat and mass transfer between impinging gas jets and solid surfaces*, *Advances in Heat Transfer*, Academic Press, New York, Vol. 13, pp. 1-60.
- [6] San, J.Y., huang, C.H., and Shu, M.H., *Impingement cooling of a confined circular air jet*, *International journal of heat and mass transfer*, 1997,Vol.40, pp 1355-1364
- [7] Adrian Bejan Allan D. Kraus, *Heat Transfer 2003 Handbook*, John Wiley & Sons, Inc., Hoboken, New Jersey, 2003
- [8] S. V. Patankar, *Numerical heat transfer and fluid flow*, McGraw Hill, New York, 1980.

Nomenclature

- d Nozzle diameter, m
- Z Distance between nozzle exit and impinging plate, m
- Z/d Dimensionless jet to target plate spacing
- V Mean velocity at jet exit, m/s
- Re Reynolds number based on jet exit diameter
 $= \rho V / \mu$
- Nu_a Average Nusselt number